Compact Linear Split Stirling Cryogenic Cooler for High Temperature Infrared Imagers

A. Veprik, S. Zehtzer, N. Pundak, S. Riabzev*

Ricor, Cryogenic and Vacuum Systems,
En Harod, 18960, Israel

*EADS Astrium LTD
Stevenage, SG1 2AS, UK

ABSTRACT

Novel high-definition night vision imagers are being enabled by new high-temperature infrared detectors that operate at elevated temperatures ranging from 95K to 200K; these have performance indices comparable with those of their 77K predecessors.

Recent technological progress towards industrial implementation of such detectors has motivated the development of microminiature split Stirling linear cryocoolers. These coolers have great potential to replace the traditionally used rotary integral Stirling coolers. Their known advantages are superior flexibility in system packaging, constant and high drive frequency, lower wideband vibration export, unsurpassed reliability, and aural stealth. Unfortunately, off-the-shelf available tactical linear coolers relying on flexural-bearing, contactless, dual-piston compressors are thus far oversized, overweight, overpowered, and overpriced as compared to their rotary competitors.

The authors report on the successful development of the smallest in the range Ricor model K527 microminiature 1W at 95K split Stirling linear cryogenic cooler. This cooler relies on a single piston externally counterbalanced linear compressor, and was designed to provide cryogenic cooling to a wide range of forthcoming infrared imagers, particularly those where power consumption, compactness, vibration, aural noise, and ownership costs are of concern.

INTRODUCTION

Infrared (IR) imagers play a vital role in the modern tactics of carrying out surveillance, reconnaissance, and targeting. By converting the thermal battlefield into dynamic visual imagery, such equipment dramatically enhances the observation and command control capabilities of the leaders of combat infantry and Special Forces.

In spite of the recent advances and widespread use of uncooled infrared detectors, it is still generally accepted that the "best technology for true IR heat detection is the cooled detector" [1]. Cold detectors are outperforming their uncooled competitors in terms of working ranges, resolution, and ability to detect/track fast moving objects in dynamic infrared scenes. The superior performance of such imagers is achieved by using novel optronic technologies along with maintaining their IR focal plane arrays (FPA) at cryogenic temperatures (77K, typically) using microminiature Stirling closed-cycle cryogenic coolers.

Cryocoolers 16, edited by S.D. Miller and R.G. Ross, Jr.

Over the past few years, industrial progress has led to the development of a new InAlSb diode technology relying on Antimonide Based Compound Semiconductors (ABCS), offering lower dark currents or higher operating temperatures (being in the 100 K region) [2]. The SWIR MCT technology [3] offers the possibility of operating a FPA at even higher temperatures, in excess of 200 K. The authors of [4] report on a 320×256 middle-wavelength infrared focal plane array based on InAs quantum-dot/InGaAs quantum-well/InAlAs barrier detector operating at temperatures of up to 200K.

The direct benefits of using such high temperature IR FPAs are the lowering of the cooling constraints, thus resulting in a simplified system design, using smaller and more cost effective, long life cryocoolers inherently consuming less electrical power and showing faster cooldown times.

Traditionally, integral rotary cryocoolers have been used for maintaining cooled IR FPAs at their optimal cryogenic temperatures. As compared to their military off-the-shelf linear competitors, they are lighter, more compact, and normally have better electromechanical performance indices. However, their inherent drawbacks, such as high wideband vibration export and limited lifespan have spurred the development of the microminiature linearly driven Stirling cryogenic coolers. An additional advantage of linear cryocoolers, as compared with their rotary rivals, should be that, at least in theory, they might operate at elevated driving frequencies without compromising their overall life span.

These novel, long-life, acoustically, and dynamically quiet cryogenic coolers, while being superior in many respects, need to be comparable to the above rotary cryocoolers in terms of bulk, power consumption, and ownership costs. Unfortunately, such coolers are still not off-the-shelf available; the existing linear tactical coolers that rely on flexural bearings and contactless dual-piston compressors are oversized, overweight, overpriced and power-thirsty, thus making them inadequate for the above purposes.

The authors report on the successful development of a novel Ricor model K527 microminiature 1W at 95 K split Stirling linear cryogenic cooler [5,6], which was designed to provide cryogenic cooling to a wide range of forthcoming infrared imagers where power consumption, compactness, vibration, aural noise, and ownership costs are of concern. In the design of the Ricor model K527 cryogenic cooler, the authors abandoned the more traditional contactless flexural bearing dual-piston compressor approach in favor of an externally counterbalanced, vibration isolated single-piston compressor. This design was made possible by eliminating the weight of one moving assembly and using novel technology and tribological wear-resistant materials for manufacturing the rubbing, tightly matched piston/cylinder liners. This has enabled a low vibration, high performance, long life and compact cryocooler for use in portable handheld, ground based and gyrostabilized IR imagers.

THERMODYNAMIC DESIGN OF CRYOGENIC COOLER

Numerical Modeling and Optimization

Computer modeling and optimization of the geometric/functional parameters was completed during the initial phase of the K527 Stirling cryocooler design. The baseline configuration was chosen with respect to its potential for providing high efficiency, compactness, robustness and low cost. The detailed cooler mechanism architecture was modeled as described below, including the temperature dependency of the displacer gap along its length.

Goal of Optimization

The optimization goal was to minimize the PV power at the cooler piston face required to deliver a nominal heat lift of 300mW at 95K at 28°C, and a maximum heat lift of 750mW at 95K at 28°C, these being consistent with a need for the minimum redundancy and reasonably fast cooldown times. A split Stirling linear cooler using a single-piston resonant compressor was chosen as the baseline configuration.

SAGE Model Description

The K527 cryocooler modeling was performed using the SAGE® environment, relying on the above defined specification and baseline configuration.

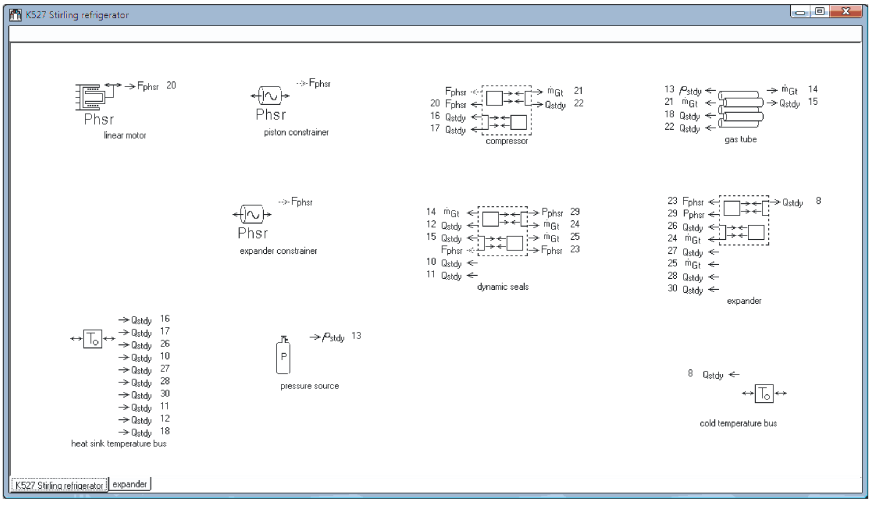

Figure 1. Screen-shot of the top level SAGE® model of K527 refrigerator

A typical screen-shot of the K527 SAGE® model is shown in Figure 1. Accurate modeling of the radial gap between the displacer and cold finger was implemented with the objective of addressing the effect of its variation associated with the temperature gradient that typically develops along the displacer length. In doing so, the displacer gap element available in SAGE® was subdivided into ten sequential sections. This allowed definition of a mean gap value in each section as a function of mean temperature and the thermal expansion coefficients of the materials involved.

In the first iteration of modeling, a very approximate model of the compressor actuator was used, as only the PV power at the piston face and the piston driving force were of interest. In subsequent iterations, after the detailed design of the linear actuator, a more accurate approach was used. In particular, the temperature compensation of the actuator coil resistance was programmed, assuming the coil is maintained 10°C above the reject temperature defined. The actuator constant coefficient was assumed to be independent of the moving magnet position, as predicted by the actuator analysis [5].

Optimization Results

The parameters shown in Table 1 were programmed to be optimized by the SAGE® routine. As explained above, the goal was to minimize the compressor PV power delivered from the piston while meeting the required cold head heat lift. The detailed cooler performance predicted for this optimal configuration is shown on a series of self-explanatory charts provided later in the section titled “Predicted Versus Experimental Performance.”

Table 1. Optimization parameters

Optimal parameters	Value
Driving frequency, Hz	75
Charge pressure, bar	13
Compressor	
Piston diameter/stroke, mm p-p	9.5/7
Spring rate, N/m	2000
Moving assembly mass, gr	35
Cold head	
Displacer diameter/stroke p-p mm	7.6/5
Spring rate, N/m	2000
Moving assembly mass, gr	10
Driving plunger dia, mm	3.8

Optimal parameters	Value
Cold head (Con't)	
Cold finger wall thickness, mm	0.08
Cold finger conductive loss, mW	145
Regenerator	
Diameter, mm	6.5
Length, mm	38.8
Screens wire diameter, mm	0.025
Porosity,%	0.665
Transfer line	
Length, mm	100
Inner diameter, mm	1.1

DESCRIPTION OF MECHANICAL DESIGN

K527 Expander Unit

The expander unit comprises a "mass-spring," pneumatically driven displacer-regenerator, as is widely accepted across the industry. Needless to say, it is favorable to design such a displacer-regenerator so that it operates it at or near its resonant frequency. The first benefit of such a resonant tuning is that the displacer stroke achieves its maximum for a given pneumatic force delivered by the compressor, or alternatively, the desired displacer stroke may be obtained at minimum pneumatic force delivery. The second benefit is that tuning the displacer to resonate delivers almost automatically the desired 90º phase angle between displacer motion and the pressure pulses arriving through the transfer line from the compression space, as is needed for producing maximum cooling [6]. The above two benefits contribute essentially to improving the displacer's expansion efficiency for a given acoustic power delivered by the compressor. Resulting from this is improved heat pumping from the expansion space to which the heat payload is thermally linked. Since the spring effect of the equivalent gaso-dynamic viscoelastic loading in the expander is negligibly small, the inertia of the moving assembly and the equivalent elasticity of the above-mentioned spring define the closeness to the resonance condition.

There are two different approaches to forming the above "spring" component. In the first approach, a helical wire spring, or, alternatively, two counter-facing preloaded helical wire springs, are arranged to support the movable displacer-regenerator assembly from the stationary housing. Using mechanical springs yields a compact design and convenient resonant tuning which appears to be almost independent of environmental temperature. The inherent disadvantages of such a design are unreliable mechanical spring connection, radiation of acoustic noise, tiny metal debris generation, and, most important, exertion of large side forces on the dynamic seals leading to excessive friction, parasitic losses, and wear and tear.

In another implementation, a "pneumatic pillow" [7] may be formed by a plunger tail cyclically protruding from the sealed rear space. This approach is widely accepted because of its compactness and almost frictionless operation. Unfortunately, the spring rate of such a pneumatic spring is a function not only of the rear space volume and plunger area, but also of the average pressure and environmental temperature. Thus, these variables have a strong influence on the above resonant frequency. An additional disadvantage is excessive overheating of the cold finger housing because of the irreversible compression losses associated with cyclic compression of the gas sealed inside this rear space that forms the "gas pillow."

In the present design, the authors capitalize on using a highly accurate double starting helix machined spring with integral retainers [8]. The high mechanical accuracy has been achieved using precise EDM machining. Figure 2 shows a schematic (a) and an external photograph (b) of the pneumatically driven expander [6].

K527 LINEAR COMPRESSOR

As is known, a single-piston compressor is a powerful source of exported vibration at its driving frequency and higher-order harmonics [9]. It is widely accepted, therefore, that a dual-piston compressor, which "should-be" dynamically counterbalanced, is the solution of choice for inherently vibration sensitive cooled IR applications. Several major cryogenic cooler vendors manufacture microminiature (below 1.5W at 77K) split Stirling cryogenic coolers comprising dual-piston,

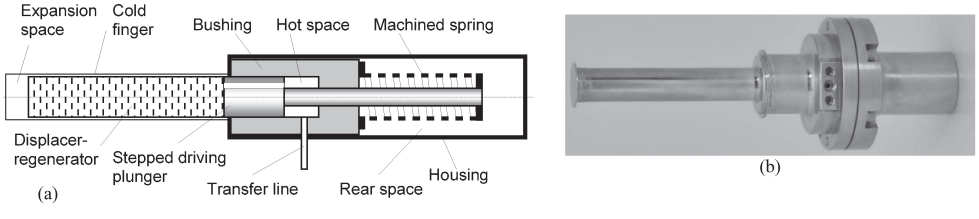

Figure 2. Schematic and external layout of a pneumatically driven expander

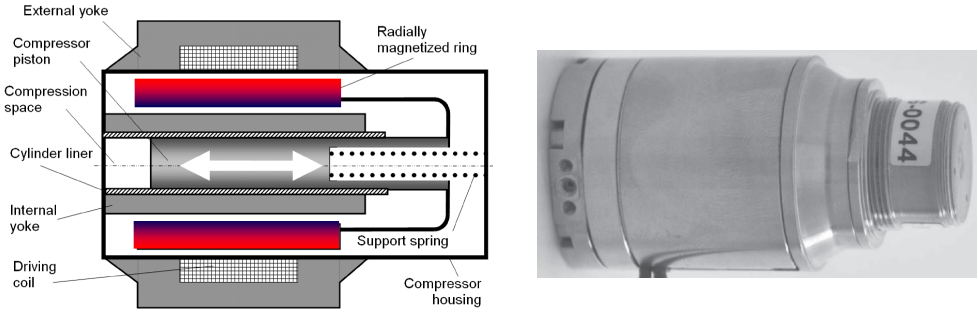

Figure 3. Schematics and external layout of a linear compressor

"moving magnet," flexural bearing compressors [10, 11]. These are achieved, however, at the expenses of size, weight, manufacturing costs, reduced electromechanical performance, and reliability. Moreover, since the sub-compressors are not entirely similar (different piston-cylinder gaps and friction forces, magnet force, driving coils resistances, etc) the residual vibration exported at the driving frequency and higher-order harmonics is not really encouraging; reaching low levels of vibration export may require additional vibration isolation, or sometimes active vibration cancellation. With this in mind, the authors have rejected the dual-piston approach in favor of a single-piston compressor design where vibration control relies on a field-proven combination of a high frequency vibration isolator, and a tuned dynamic absorber, as explained, for example, in [12].

The single-piston K527 linear compressor is driven by a resonant "moving magnet" actuator. This allows it to obtain a high coefficient of performance [5,6] and also allows the driving coil to be separated from the working agent (Helium, typically), thus preventing the cooler interior from being contaminated by outgassing products originating from the wire insulation varnish. Having the coils outside also eliminates the need for flying leads and potentially leaking feedthroughs. It is also important to note that in such an approach, heatsinking the intrinsic copper losses from the externally located drive coil is much improved.

Figure 3 shows a schematic (a) and external photograph (b) of such a compressor. In Figure 3a, the radially magnetized ring is placed movably between the stationary internal and external armature yokes, which are made of a magnetically soft material. The above yokes are shaped in such a fashion so as to accommodate the driving coil carrying the AC current and to provide for the quasi uniform distribution of the magnetic flux within the working air gap without oversaturating the yoke's material [5,6].

The above magnetic ring is bonded upon the magnet form, which is, in turn, rigidly attached to the compression piston, arranged so as to slide freely inside the tightly matched cylinder liner being placed inside the internal yoke.

For the sake of compactness, a double starting helix machined spring, connecting the movable piston and stationary housing is placed inside the piston. A sliding piston/cylinder pair design provides important improvements in performance, compactness, manufacturing costs, ease of assembly and maintenance. It replaces the "contactless" approach that relies on flexural bearings and accurate (sometimes robotic) alignment and assembly [11]. The piston and cylinder liners are tightly matched to 4μm radial clearance and are made of a special tribological material.

As described above, using a precise double starting helix machined spring allows improved alignment and low friction forces along with eliminating metal debris generation. An additional advantage of this approach is that the piston-cylinder sleeves may be matched more tightly as compared to the above contactless design; this results in a substantial decrease in blowby losses. This decision to abandon the flexure bearing design is based on the proven technology used currently in the Ricor model K529N cryogenic cooler, where in the course of the accelerated life test the experimental cooler accumulated in excess of 27,500 working hours (equivalent to 45,000 hours under standard test profile). When investigating this experimental cooler's failure, it appeared that an electrical short in the driving coil happened due to overheating of the inappropriately chosen var-

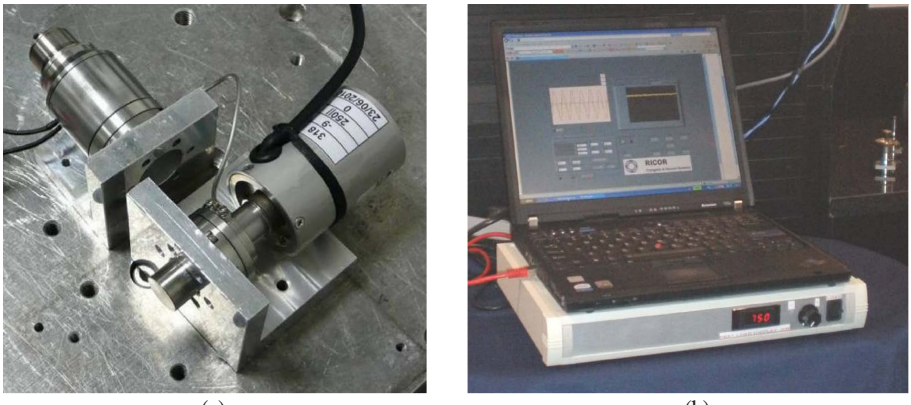

(a) (b)

Figure 4. Experimental setup

nish type [13]. The "post mortem" inspection revealed that the outer diameter of the piston and inner diameter of the cylinder liners were still within the manufacturing tolerances, and that the working surfaces were free of abrasive scratches and wear.

Based on the theoretical analysis of [5,6], optimizing the "moving magnet" linear actuator requires maintaining the ratio R/α^2 (R and α stand for the driving coil resistance and force/current constant, respectively) at the lowest possible level. In an ideal case this means increasing the "copper volume" and magnetic flux in the air gap along with using low resistive wire for making the driving coil. No less important in this regard, is to also provide for effective heatsinking of the Joule heating originating from the drive coil.

EXPERIMENTAL MAPPING

Experimental Setup

The experimental testing involved monitoring and data acquisition of electrical quantities like voltage, current and power consumed by the linear compressor, cold finger temperature, piston and displacer strokes, pressure pulse, and heat load applied to the cold finger tip.

Figure 4 shows pictures of the experimental setup. In Figure 4(a), the compressor and expander units of the K527 cryogenic cooler are placed at 90 degrees to each other on the Kistler 9272A dynamometer. This enables simultaneous monitoring and data acquisition of the vibration export produced by the two above components.

Figure 4(b) shows the test bench and the dedicated notebook computer that provides closed-loop temperature control operation of the cryocooler. The basic function of the test bench is to monitor the cold finger temperature and produce a drive voltage of constant frequency for the compressor unit. The magnitude of the voltage is varied to maintain the cold tip temperature at the prescribed level under different working conditions.

Figure 5 shows a schematic of the experimental setup. The pressure P on the piston face is monitored by a Kistler Type 603B1 pressure transducer placed inside a special adaptor, thus making it a part of the transfer line. The electrical signals from the above pressure sensor P, motor current I, and vibration forces F_c (compressor) and F_e (expander) are conditioned in the Bruel & Kjaer Nexus charge amplifier and then fed to the multichannel Data Physics Quattro Signal Analyzer for data acquisition and digital signal processing.

Mapping and Post-Processing

The parameters of the K527 prototype unit were mapped experimentally as shown in Table 2, by varying the coldtip electrical heat load while in temperature-controlled mode. Since the above vibration forces F_c and F_e are products of the moving masses and accelerations, as explained in [9], these signals were used for noninvasive monitoring of the piston and displacer motion.

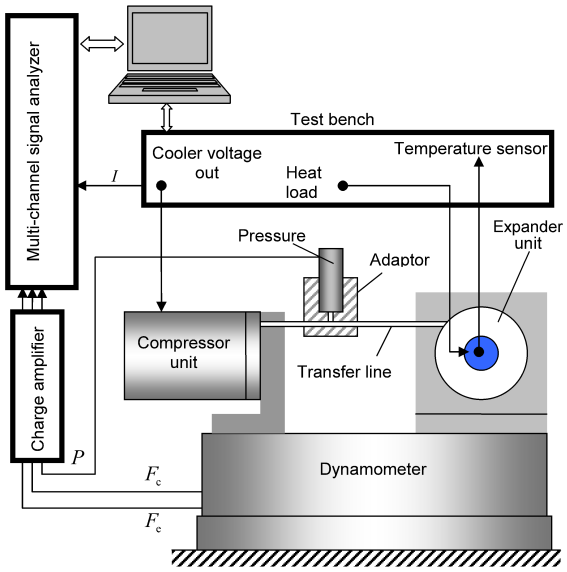

Figure 5. Schematic of experimental setup

Table 2. Experimental mapping outcomes

Q_{net} mW	W_{in} W AC	I A rms	F_c / F_e N	P bar	$P \measuredangle F_c$ deg	$P \measuredangle F_e$ deg
0	2.3	1.04	8.8/1.5	0.75	-140	-31
100	3.7	1.34	10.7/1.9	0.98	-139	-29
200	5.3	1.63	12.3/2.2	1.13	-137	-27
300	7.4	1.95	14/2.5	1.39	-136	-26
400	9.6	2.25	15.3/2.8	1.55	-135	-24
500	12.7	2.65	17.2/3.1	1.85	-135	-22
600	16	3.01	18.7/3.4	2.06	-134	-20
700	20	3.40	20.4/3.6	2.27	-134	-18

Further, the recorded data were post-processed, aiming at calculation of the piston and displacer magnitudes, phase lag between them, and the PV power at the piston face. The postprocessing assumption was that the measured dynamic signals were of a purely harmonic shape. In addition, the actuator coil resistance loss was identified using the experimental results.

In Table 2, representing raw data, Q_{net} stands for added heat load; W_{in} – power consumption; I – motor current; F_c and F_e - vibration export produced by compressor and expander, respectively; P – pressure on the piston face; $P \measuredangle F_c$ - angle between pressure and compressor vibration force; $P \measuredangle F_e$ angle between pressure and expander vibration force.

Further, we use the following notations and formulae: ω - driving angular frequency; m_p - piston assembly mass; m_d - displacer assembly mass, d_p - piston diameter; $A_p = \pi d_p^2/4$ - piston face area; $x_p = F_c/m_p\omega^2$, $x_d = F_c/m_d\omega^2$ - piston and displacer magnitudes; $x_p \measuredangle x_d = P \measuredangle F_p - P \measuredangle F_d$ - phase lag between piston and displacer positions; $dV = \omega x_p A_p$ - volumetric speed amplitude; $P \measuredangle dV = P \measuredangle F_p + 90°$ - phase lag between pulse oscillations and compressor volumetric speed; $W_{PV} = PdV \cos(P \measuredangle dV)$ - PV power at piston face; $W_{coil} = I^2R$ – resistance loss in actuator coil. Table 3 summarizes the results of the postprocessing done using the above equations.

Table 3. Postprocessing outcomes

X_p, mm	X_d, mm	$x_p \angle x_d$, deg	dV, m^3/s x 10^{-5}	$P \angle dV$ deg	W_{pv} W	W_{coil} W
1.1	0.7	-109	3.8	-50	0.9	0.4
1.4	0.9	-110	4.6	-49	1.5	0.7
1.6	1	-110	5.3	-47	2	1
1.8	1.1	-110	6	-46	2.8	1.4
2	1.3	-111	6.6	-45	3.5	1.9
2.2	1.4	-113	7.4	-45	4.7	2.7
2.4	1.5	-114	8.	-44	5.8	3.4
2.6	1.6	-115	8.8	-44	7	4.4

PREDICTED VERSUS EXPERIMENTAL PERFORMANCE

The purpose of the experimental testing was to compare the actual cooler performance with the outcomes of the theoretical predictions based on the above computer modeling. This testing was undertaken primarily to validate the computer model with the purpose of scaling the cryogenic cooler to different working conditions. As a result, a number of performance charts were generated using the SAGE® model and further superimposed on the experimental data.

All the validated parameters are shown graphically in Figures 6 and 7 versus PV power available at the piston face. This sort of data presentation was chosen to allow a virtual separation between thermodynamic and electromechanical circuits in the modeled cryocooler.

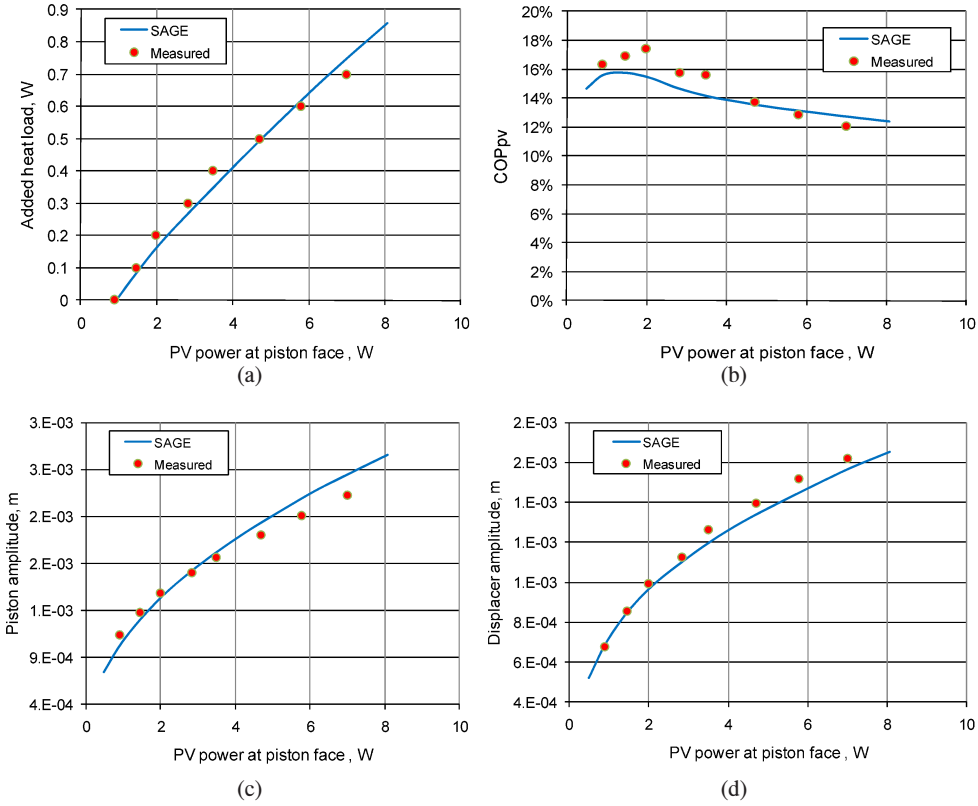

Figure 6. Verification charts of K527 SAGE® model versus experimental data.

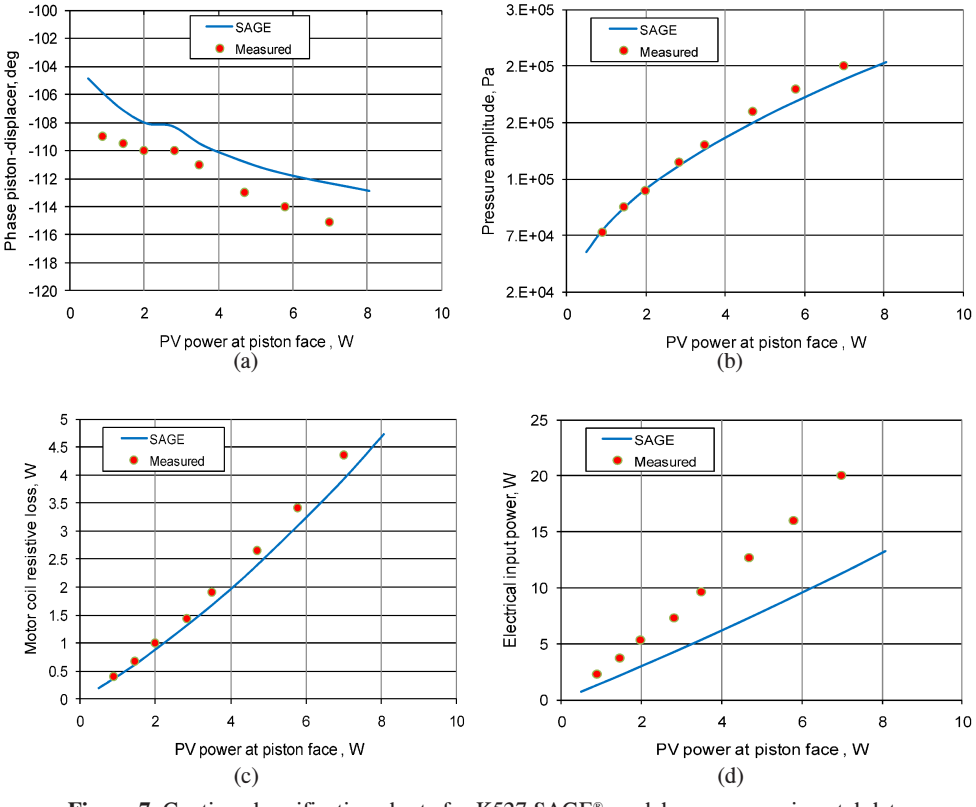

Figure 7. Continued verification charts for K527 SAGE® model versus experimental data.

From the eight charts in Figures 6 and 7, it is clear that the modeled data agree reasonably well with the measured parameters. The only exception is the input power of the compressor actuator, which does differ noticeably from the experimental data. Concluding the verification work, it is obvious that the SAGE® model does reasonably reflect the reality in terms of thermodynamics, despite the noticeable discrepancy in the electrical input power. The discrepancy is most likely to be related to iron and eddy-current losses in the compressor actuator, which could not be precisely addressed in the SAGE® environment. From Figure 7d, further essential improvements may be available by redesigning the linear actuator.

Cooler Study at the Point of Optimal Design

As was mentioned above, the K527 cryogenic cooler has been optimized to maintain a 750mW payload load (e.g. infrared FPA) at 95K, while rejecting its heat at a temperature of 28°C. Since the cooler is intended for operation over the wide range of reject temperatures, and therefore heat lifts, it was important to evaluate the performance of the cooler working at 95K over the entire range of working conditions. Figure 8 shows the typical dependence of the maximum added heat load on environmental temperature at 45W AC max. From Figure 9, this cooler might be characterized as 1W at 95K. During the typical cool down test from 290K to 95K, a thermal mass of approximately 200 J was affixed to the cold finger tip to mimic the mass of a real detector. During the 45s soft start the power consumption was gradually increased from 7 to 15W AC. Further increases up to 18W AC took place at constant driving voltage. Figure 9 portrays the time variation of the cold tip temperature and the input power during the above test. The data indicate a less than 2.5 min cool-down time and a smooth transition into the controllable mode. The cooldown time may be further improved by shortening the soft start phase and increasing the maximum power up to 30W AC.

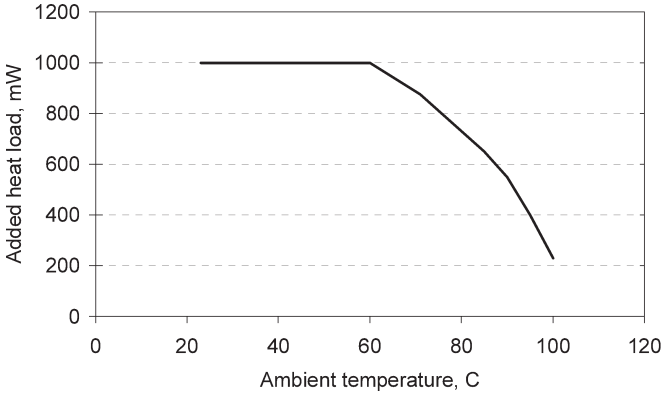

Figure 8. Maximum cooling capacity at different ambient temperatures

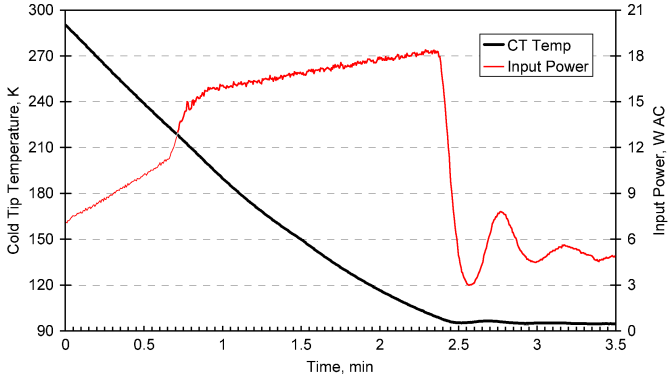

Figure 9. Typical cool down test

Comparison with Other Coolers

Table 4 compares dimensions, weights, vibration export and MTTFs of typical dual-piston compressors of microminiature split Stirling cryocoolers offered by the world's leading vendors. In the table, the last three rows present the Ricor model K527 single-piston compressor in different modifications; this reveals a clear advance in all the listed parameters. The conservatively predicted MTTF in excess of 30,000 hours relies on experimental data obtained during life testing of the similar Ricor model K529 cryogenic cooler [13], which achieved 45,000 operational hours. It is important to remind the reader, that the linear compressor of the K529 cooler is driven by a "moving coil" actuator, and therefore has the drive coil inside the Helium charged interior. Thus, it also has flying leads, feedthroughs, and problematic heat sinking. The K527 compressor is free of the above disadvantages, and therefore has a great potential for an even longer MTTF. Actual life testing is just beginning, the authors will report on the outcome as soon as it is available.

Further, from Table 4, the vibration export produced by a vibration mounted K527 compressor is comparable with that of the dual-piston designs; adding a 100gr tuned dynamic absorber reduces the vibration export to typically 0.03N, which is an order of magnitude lower than that of the listed rivals. Details of the design and attainable performance of the vibration reduction interface, which relies on a combination of high frequency vibration mount and tuned dynamic absorber, are disclosed in [6].

Self-explanatory, Figure 10 compares the power consumption of the above coolers operating in temperature-control mode (77 K with 23°C heatsink temperature) for different heat lifts. The marked points represent the performance of "competitors," while the bold solid line represents that of the Ricor model K527 cooler.

Table 4. K527 vs competitors

VENDOR / MODEL	LXOD mm	WEIGHT gr	VIBRATION N	MTTF HOURS
AIM / SF070B	115X45	1000		>20,000
AIM / SL070A	129X45	940		>8,000
AIM / SL100	122X60.5	2000		>4,000
AIM / SF100A	119X60.5	1600		>20,000
AIM / SF100B	122X57	1600		>20,000
CARLETON / LC1040	142X45	1000	1.35	>8,000
CARLETON / LC1056	120X45	1000	1.35	>8,000
CARLETON / LC1062	120X45	1000	1.35	>10,000
CARLETON / LC1055	120X46	1000	1.35	>8,000
CARLETON / LC1047	120X60	1700	2.25	>8,000
RAYTHEON / 7050	120X51	1300	2.25	>4,000
RAYTHEON / 7049/7051	203X45	1250	2.25	>2,500
RAYTHEON / 7052	120X52	1300	2.25	>5,000
RAYTHEON / 7060	120X40	450	1.35	>4,000
RAYTHEON / 7062&196S	114X33.5	400	1.35	>4,000
RAYTHEON / 7070	120X45	600	1.35	>4,000
THALES / LSF95-80/87/88/89/97/99	122X60	1500	2.5	>20,000
THALES / UP70-80/87/88/89	122X55	1500	2.25	>4,000
THALES / UP70-86/97	120X44	1150	2.25	>4,000
THALES/UP8497	125X35	450	2.25	>15,000
L-3 / B500C		400	0.9	>4,000
L- 3 / B600		1000	0.9	>4,000
L-3 / B1000		1600	2.25	>4,000
BEI / B602	102X45	800	2.25	
DRS / 1W LINEAR COOLER	116X60.5	1600	2.25	
RICOR / K527	63X33.5	200	11	>30,000
RICOR / K527 + 30HZ VIBRATION MOUNT	63X33.5	220	2	>30,000
RICOR / K527 + 20HZ VIBRATION MOUNT	63X33.5	221	0.9	>30,000
RICOR / K527 + 30HZ VIBRATION MOUNT +TUNED DYNAMIC ABSORBER	93X33.5	300	0.03	>30,000

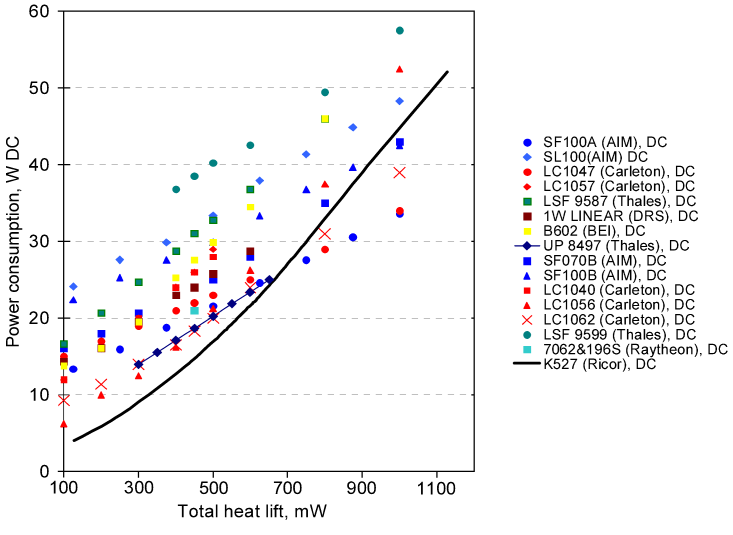

Figure 10. Comparison of microminiature linear split Stirling cryogenic coolers

CONCLUSIONS

The novel Ricor model K527 1W at 95K cryogenic cooler has been presented. It is comprised of a single-piston compressor driven by a resonant "moving magnet" actuator and uses a pneumatically-driven resonant expander. The decision to abandon the fashionable dual-piston and contactless compressor approach allowed a drastic simplification of the mechanical design. This resulted in a smaller, lighter, more power efficient, and reliable cryogenic cooler, as compared with available COTS linear rivals.

This cryogenic cooler is ideally suited for a wide range of forthcoming high-temperature electro optical instrumentation like portable handheld cameras, thermal weapon sights, ground fixed and vehicle mounted surveillance cameras, gyrostabilized imagers, etc.

REFERENCES

1. Gething, M., J., "Seeking the heat in the night," Jane's International Defense Review, 38, 42-47 (2005).
2. Glozman, A., Harush, E., Jacobsohn, E., Klin, O., Klipstein, P., Markovitz, T., Nahum V., Saguy E., Oiknine-Schlesinger, J., Shtrichman, I., Yassen, M., Yofis, B. and Weiss, E., "High performance InAlSb MWIR detectors operating at 100K and beyond," *Proc. SPIE* 6206, 62060M (2006).
3. Tribolet, P., Costa, P., Fillon, P., Manissadjian, A. and Chorier, P., "Large staring arrays at Sofradir," *Proc. SPIE* 4820, 418 (2003).
4. Tsao, S., Lim, H., Zhang, W. and Razeghi, M., "High operating temperature 320×256 middlewavelength infrared focal plane array imaging based on an InAs/InGaAs/InAlAs/InP quantum dot infrared photodetector," *Appl. Phys. Lett.* 90, 201109 (2007).
5. Veprik, A., Vilenchik, H, Riabzev, S. and Pundak, N., "Microminiature linear split Stirling cryogenic cooler for portable infrared imagers," *Proc. SPIE* 6542, 65422F (2007).
6. A. Veprik, S. Zechtzer and N. Pundak, "Split Stirling linear cryogenic cooler for a new generation of high temperature infrared imagers," *Proc. SPIE* 7660, 76602K (2010).
7. Walker, G., *Cryogenic coolers*, Plenum Press, New York (1983).
8. Curven, P.,W., Newell, R.,V, "Resonant piston pump," USA Patent #3,588,291 (1971).
9. Riabzev, S., V., Veprik, A.,M. and Pundak, N., "Technical diagnostics of linear split Stirling cryocooler through the analysis of self-induced forces," *Adv. in Cryogenic Engineering*, Vol. 47B, Amer. Institute of Physics, Melville, NY (2002), pp. 1141-1148.
10. Mullie, J.,C., Bruins, P.,C., Benschop, T. and Meijers, M., "Development of the LSF95xx 2nd generation flexure bearing coolers," *Proc. SPIE* 5783, 178 (2005).
11. Rühlich, I., Wiedmann, T., Mai, M. and Rosenhagen C., "Flexure bearing compressor in the onewatt linear (OWL) envelope," *Proc. SPIE* 6542, 65422I (2007).
12. Veprik, A., M., Babitsky, V.,I, Pundak, N. and Riabzev S., "Vibration control of linear split Stirling cryogenic cooler for airborne infrared application," *Journal of Shock and Vibration* 7(6) (2000), pp. 363-379.
13. Nachman, I., Veprik, A. and Pundak, N., "Life test result of Ricor K529N 1W linear cryocooler," *Proc. SPIE 6542*, 65422G (2007).
14. Gedeon D., *Sage Pulse Tube Model-Class Reference Guide*, Gedeon Associates (1999).
15. Veprik, A.,M., Babitsky, V.,I., Pundak, N. and Riabzev, S., "Vibration control of linear split Stirling cryogenic cooler for airborne infrared application," *Journal of Shock and Vibration* 7(6) (2000), pp. 363-379.